Intermolecular Interactions

International Edition: DOI: 10.1002/anie.201803363
German Edition: DOI: 10.1002/ange.201803363

Hole Mobility Modulation in Single-Crystal Metal Phthalocyanines by Changing the Metal–π/π–π Interactions

Hui Jiang[+], Peng Hu[+], Jun Ye[+], Rakesh Ganguly, Yongxin Li, Yi Long, Denis Fichou,* Wenping Hu,* and Christian Kloc**

Abstract: *Weak intermolecular interactions in organic semiconducting molecular crystals play an important role in determining molecular packing and electronic properties. Single crystals of metal-free and metal phthalocyanines were synthesized to investigate how the coordination of the central metal atom affects their molecular packing and resultant electronic properties. Single-crystal field-effect transistors were made and showed a hole mobility order of ZnPc > MnPc > FePc > CoPc > CuPc > H_2Pc > NiPc. Density functional theory (DFT) and 1D polaron transport theory reach a good agreement in reproducing the experimentally measured trend for hole mobility. Additional detail analysis at the DFT level suggests the metal atom coordination into H_2Pc planes can tune the hole mobility via adjusting the intermolecular distances along the shortest axis with closest parallel π stackings.*

Organic semiconducting molecules with highly extended π–π stackings and enhanced intermolecular interactions are expected to give rise to high performance for organic electronics.[1] As a typical example, phthalocyanine is a conjugated macrocycle with 18 π electrons distributed within a large plane,[2] and central metal-atom coordination[3] plays a significant role in affecting their electronic structures and applications.[4] For example, the chemical sensitivity of metal phthalocyanine (MPc) gas sensors can be changed by selecting different metal atom coordination.[5] Organic magnetic and spin devices are observed in MPcs with specific metal atom coordination.[6] Also, different MPcs will give different solar cell performance.[4b,7] The previous results indicate that some MPcs and derivatives have been shown to be good candidates for organic electronics owing to the advantages of low fabrication cost, high mobilities, and excellent air stabilities.[8] Although MPcs have a broad application range, the relationship between central metal atom coordination and the π-plane of metal-free phthalocyanine (H_2Pc) is still an open question. Three questions should be addressed: 1) Will the electronic properties of H_2Pc be modified by the introduction of a central metal atom? Hydrogen bonding dominates the intramolecular interaction in H_2Pc while the charge transfer and oxidation of the central metal atoms mainly contributes to the properties in MPcs.[5b,9] Some results supported the oxidation of metal atom coordination induced the semiconductor behavior[10] while H_2Pc thin films showed hole transport in a vertical magnetic field.[11] Also, it is unclear if the metal atom coordination of H_2Pc results in worse or better electronic performance. 2) Is there a significant difference between different metal atom coordination? Many previous theoretical calculations revealed that different MPcs showed identical electronic structures and the difference between metal atoms could be ignored.[12] However, many experimental results based on different MPcs showed different field-effect mobilities.[13] It is necessary to use single crystal[14] rather than thin films since grain boundaries, defects, and dislocations would also affect material properties greatly. Furthermore, MPc molecules are either totally planar (CuPc, CoPc, ZnPc, etc.),[8e,13c,e,15] or distorted (SiPc),[16] or V-shaped structures (TiOPc, VOPc, etc.).[8a,c,17] Therefore, the prediction of transport properties from one MPc to another reveals to be difficult. 3) What is the critical parameter

[*] Dr. H. Jiang,[+] Dr. R. Ganguly, Dr. Y. Li, Prof. D. Fichou
School of Physical and Mathematical Sciences
Nanyang Technological University
637371 Singapore (Singapore)
E-mail: jianghui@ntu.edu.sg
DenisFichou@ntu.edu.sg

Dr. H. Jiang,[+] Dr. P. Hu,[+] Dr. Y. Long, Prof. C. Kloc
School of Materials Science and Engineering
Nanyang Technological University
639798 Singapore (Singapore)
E-mail: ckloc@ntu.edu.sg

Dr. J. Ye[+]
Institute of High Performance Computing
Agency for Science, Technology and Research
138632 Singapore (Singapore)

Prof. D. Fichou
Sorbonne Universités, UPMC Univ Paris 06, UMR 8232, Institut Parisien de Chimie Moléculaire
75005 Paris (France),
and
CNRS, UMR 8232, Institut Parisien de Chimie Moléculaire
75005 Paris (France)

Prof. W. Hu
Tianjin Key Laboratory of Molecular Optoelectronic Sciences, Department of Chemistry, School of Science
Tianjin University and Collaborative Innovation Center of Chemical Science and Engineering (Tianjin)
Tianjin 300072 (China)
E-mail: huwp@tju.edu.cn

[+] These authors contributed equally to this work.

Supporting information and the ORCID identification number(s) for the author(s) of this article can be found under: https://doi.org/10.1002/anie.201803363.

governing the charge transport in MPcs? Although some previous reports studied the central metal atom coordination in affecting the electronic structures and gas sensing properties,[5a,b] no systematic experimental studies have been made on the weak intermolecular interactions during the metal atom coordination and how it contributes to charge transport. In an attempt to better understand the contribution of the metal atom on the transport properties of MPc molecules, herein we investigate H_2Pc and a series of planar MPc (M = Cu, Co, Zn, Fe, Ni, Mn) molecules in the form of single crystals. Also, light has been shed from theoretical calculations to understand the origin of the semiconducting properties of MPcs and the function of the coordination of different metal atoms in affecting the electronic properties and intermolecular interactions of MPcs.

Single crystals of H_2Pc, CuPc, CoPc, ZnPc, FePc, NiPc, and MnPc were grown using physical vapor transport method.[18] The molecular structures and optical images of H_2Pc and MPcs are illustrated in Figure 1. The metal atom is located at the central position of H_2Pc π-plane, and the

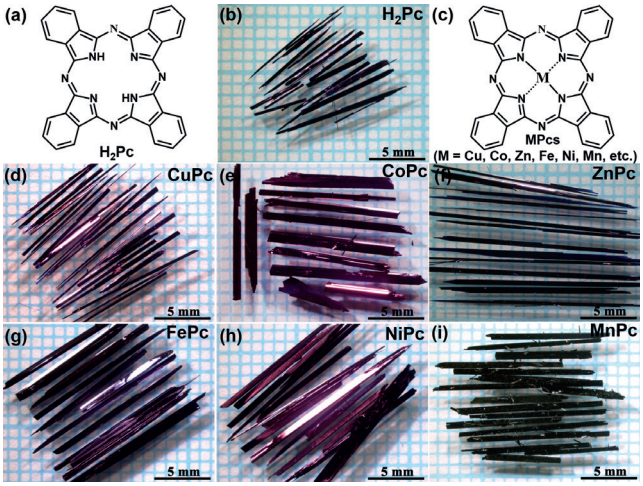

Figure 1. Molecular structures of a) H_2Pc and c) MPcs. Optical images of b) H_2Pc, d) CuPc, e) CoPc, f) ZnPc, g) FePc, h) NiPc, and i) MnPc single crystals.

coordination number for the studied MPcs is two, which means two electrons form the coordinate bonds. The crystal size of H_2Pc and MPcs can range from micrometers to centimeters via precise control of single-crystal growth parameters.[18] All H_2Pc and MPcs are violet except MnPc which is black. It means that MnPc has a lower band gap compared to H_2Pc and the other MPcs (the calculated frontier molecular orbitals of the studied H_2Pc and MPcs, see Figure S11 in the Supporting Information). Single-crystal structures were determined by single-crystal X-ray diffractometer.[26] The seven crystals (H_2Pc, CuPc, CoPc, ZnPc, FePc, NiPc, and MnPc) are of $P2_1/n$ space groups and very similar to each other for both 100 K (Table S1–S2) and room temperature (Table S3–S4). These results suggest there is no phase transition from low temperature to room temperature for all studied H_2Pc and MPcs systems.

Transmission electron microscopy (TEM) and selected area electron diffraction (SAED) were used to determine the crystal growth direction along the ribbon as shown in Figure 2. Micro-ribbon single crystals of H_2Pc and MPcs were in situ grown on the copper grid with supporting films by physical vapor transport method. The diameters of the individual crystals can be changed from few tens of nanometers to few hundreds of nanometers. The corresponding SAEDs reveal that the preferable crystal growth directions of H_2Pc and MPcs are [010], which is precisely the shortest axis (*b* axis) of the single crystals.

In our studies, H_2Pc and MPcs are all planar structures, and the metal atoms are located at the center position of the single crystals. The difference among the seven single crystals is focused on the spacing between two parallel planes ($d_{spacing}$) and the tilt angle along the shortest *b* axis as shown in Figure S1. The $d_{spacing}$ of H_2Pc is 3.2570 Å, and the tilt angle

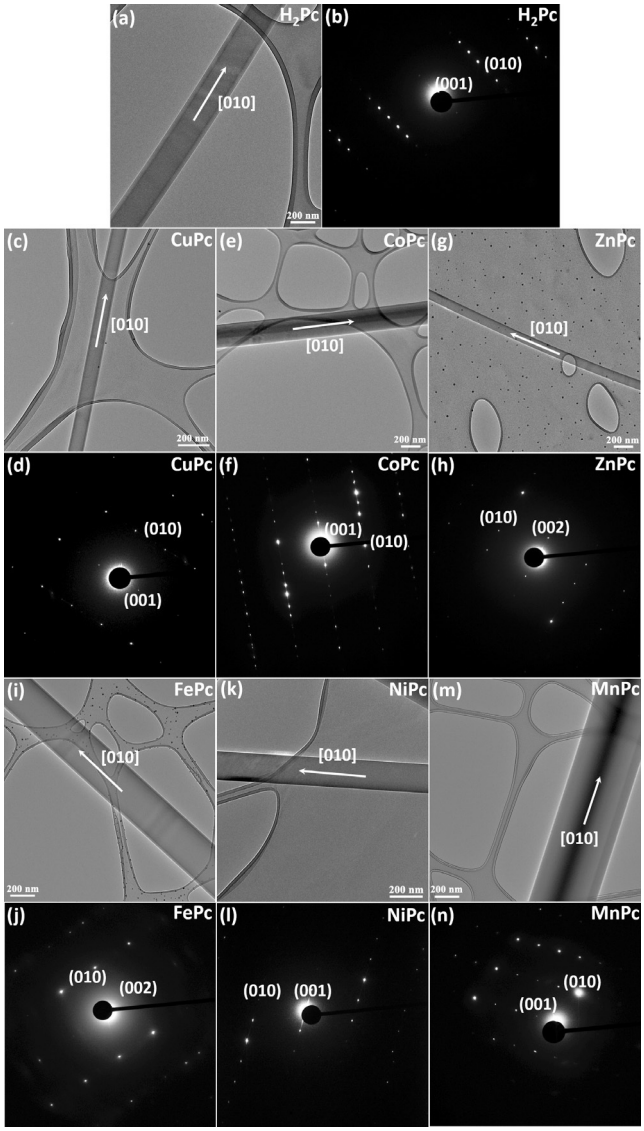

Figure 2. TEM images of a) H_2Pc, c) CuPc, e) CoPc, (g) ZnPc, i) FePc, k) NiPc, and m) MnPc. The corresponding SAED patterns of b) H_2Pc, d) CuPc, f) CoPc, h) ZnPc, j) FePc, l) NiPc, and n) MnPc.

along the [010] direction is 43.784°. When different metal atoms are coordinated with H_2Pc molecules, the interaction between the metal atoms and H_2Pc makes both the $d_{spacing}$ and the tile angle changed. Thereinto, the maximum $d_{spacing}$ is equal to 3.2970 Å in NiPc while the minimum $d_{spacing}$ is 3.1731 Å in MnPc. The smallest tilt angle along *b* axis is 41.139° for ZnPc while the largest tilt angle along *b* axis is 44.445° for NiPc (Figure S1).

How do we define the function of different metal atom coordination in MPcs? The metal atom coordination makes the molecular structure of H_2Pc slightly changed. Single-crystal field-effect transistors (SCFETs) based on individual micro-ribbons of H_2Pc and MPcs (M = Cu, Co, Zn, Fe, Ni, and Mn) were made to study the charge transport properties along the *b* axis. Micro-ribbons single crystals were in situ grown on the octadecyltrichlorosilane (OTS)-modified SiO_2/Si substrate. Then gold electrodes were thermally evaporated on the top surface of single crystals using the copper grid as the mask. SCFETs were fabricated and characterized under ambient environment. The results show that both H_2Pc and MPcs are hole transport properties and the mobilities of both H_2Pc and MPcs are greater than 0.1 $cm^2 V^{-1} s^{-1}$. Furthermore, with decreasing of the intermolecular distance of MPcs, the hole mobilities of MPcs are increased gradually with decreasing intermolecular distances (Figure 3, we selected the crystal thickness ranges from 50 nm to 500 nm for both H_2Pc and MPcs so that we can try to decrease the influence of access resistance.[19]). The optical images, atomic force microscope (AFM) images, device characteristics, and the statistics of H_2Pc and MPcs devices are also shown in Figure S2–S8.

Experimental results of intermolecular distance-dependent hole mobility in the H_2Pc and MPcs systems suggest the interesting role of central metal atoms. The single crystals grown from experiments also offer an ideal platform for theoretical study. To gain insights into the mechanistic point of view, we performed density functional theory (DFT) based calculations in conjunction with a 1D polaron transport model,[20] and the detail information of theoretical calculations are listed in the Supporting Information (Figures S11–S21, Tables S5–S9). With the parameters listed in Table S5 determined from DFT calculations, we can reach a good

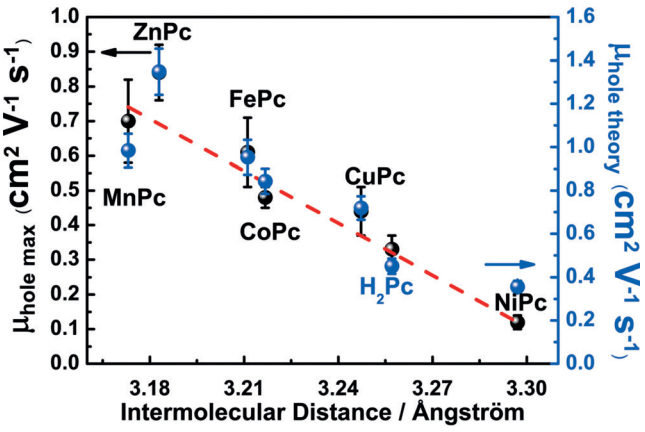

Figure 3. The measured (black) and theoretically (blue) calculated hole mobility dependence of intermolecular distance in H_2Pc and MPcs single crystals.

qualitative (or semi-quantitative) agreement of hole mobility with experiments as shown in Figure 3. The calculated values of hole mobility have been systematically overestimated compared to the experimental data, but it may be understood as a result of different defect levels and accuracy in calculating for model parameters using DFT level theory. It is generally accepted that charge transfer integral in organic semiconducting crystal systems is one of the dominating factors to control the charge transport properties. The charge transfer integral is very sensitive to the intermolecular distance and orientation between two neighboring molecules in organic crystals. It is clear from experimental crystal structures in Figure S1 that the relative orientation of the neighboring MPc molecules is nearly fixed. Thus, the role of intermolecular distance becomes critically dependent on the central atoms and their intermolecular interactions. Further insights can be gained from detail analysis of noncovalent interactions (NCI) and "quantum theory in atoms and molecules" (QTAIM)[21] in the MPc systems. Such information has been revealed from the reduced density gradient isosurfaces (RDG) and bond critical points (BCP) in H_2Pc and MPcs dimers (detail information can be found in the Supporting Information, Figures S13–S16 and Tables S6–S9), showing a strong variation of attractive interaction energies with central metal atoms. Generally, the interactions energies from BCPs $E^{Dimer}_{int(BCP)}$ follow the order of MnPc > ZnPc > CoPc > CuPc > FePc > NiPc > H_2Pc. ZnPc and MnPc exhibit strongest attractive intermolecular interactions compared to the others as suggested in Figure 4. The $E^{Dimer}_{int(BCP)}$ in these systems are almost doubled if compared to the reference H_2Pc system (ca. 80 $kJ\,mol^{-1}$ vs. ca. 43 $kJ\,mol^{-1}$). Therefore, smaller intermolecular distances in these MPcs can be related to a much stronger attractive interaction in these systems. Consequently, the hole transfer integrals (t_h) in ZnPc and MnPc are significantly higher (ca. 40 meV vs. ca. 25 meV) than the reference H_2Pc system that has no central metal atoms. Interestingly, metal atom-pyrrole N interactions [M···π(N) interactions] are observed in most cases with BCP presented in-between the metal atoms and pyrrole nitrogen atoms except for FePc as shown in both Figures S13–S16 and Tables S6–S9. Instead, we observed cage critical points (CCP) presented in the case of FePc, indicating Fe atoms are not likely to interact with pyrrole nitrogen atoms in neighboring molecules as other M atoms do. This is also supported by a hole in the RDG isosurface of FePc around the CCPs. Similarly, H_2Pc has no intermolecular M-N interactions also shown to have $E^{Dimer}_{int(BCP)}$ values close to FePc, thus leading deviation from the trend in Figure 4. If we add approximately 10 $kJ\,mol^{-1}$ energy to the $E^{Dimer}_{int(BCP)}$ values for both H_2Pc and FePc, we would expect to boost them to the points that are close to the consistent trend observed in Figure 4, which shows the importance of intermolecular M–N interactions in other MPc systems. Both MnPc ($E^{BCP}_{Mn\cdots\pi(N)} \approx 10\ kJ\,mol^{-1}$) and CoPc ($E^{BCP}_{Co\cdots\pi(N)} \approx 5\ kJ\,mol^{-1}$), especially MnPc exhibits stronger M···π(N) interactions compared to NiPc, ZnPc, and CuPc that are exhibiting M···π(N) interactions energy at the same level of π···π interactions ($E^{BCP}_{M\cdots\pi(N)} = \approx 4.5\ kJ\,mol^{-1}$). Stronger interactions in both MnPc and CoPc for M···π(N) type of interaction can be linked to their ground state metal atom d-

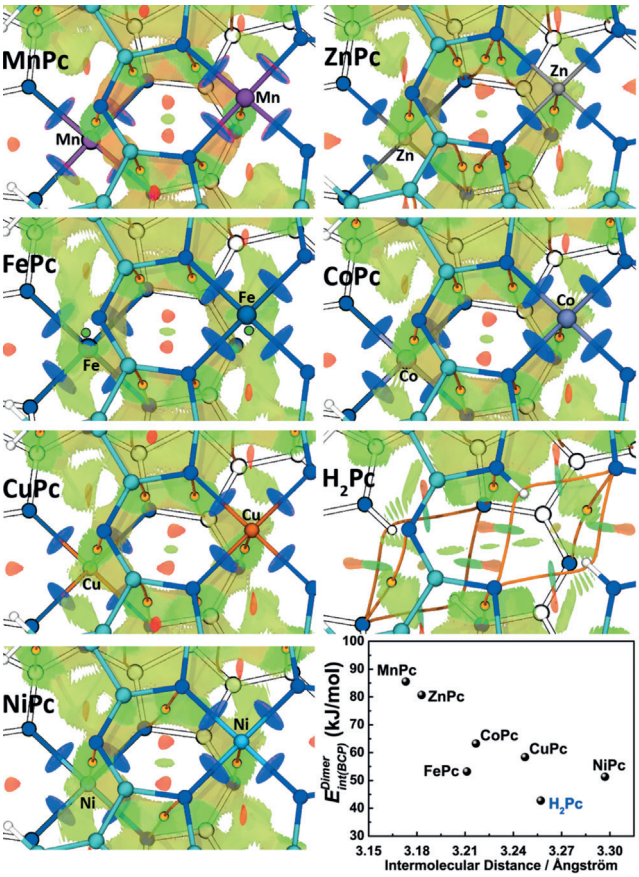

Figure 4. Expanded topology analysis results of closest parallel packed dimers in H_2Pc and MPcs with colored RDG isosurfaces (isovalue = 0.4 a.u.) against Sign(λ_2)*ρ values, showing van der Waals interaction is the dominating one in these molecular dimers. Full images of these results are given in Figures S13 to S16. The color scheme is shown Figure S13. BCPs (only intermolecular ones are shown) and respective critical paths (CPs) are colored in orange. Specifically, the cage critical point (CCP) for the case of FePc is colored in green. C cyan, H white, and N blue, in the upper MPc molecules. The lower MPc molecules are colored in white with only N atoms in blue and metal atoms in their respective colors. The interaction energies $E^{Dimer}_{int(BCP)}$ calculated from the electronic properties of the BCPs against intermolecular distances are also plotted on the lower right panel.

electron configuration with singly occupied dz^2 orbital close to their a_{1u} ligand HOMO (the highest occupied molecular orbital; Figure S11).[22] Besides M···π(N) interactions, the intermolecular π(N)···π interactions (determined from the central BCPs shown in the zoomed-in figures of NCI and QTAIM analysis results in Figure 4) exhibit interesting symmetrical pattern as suggested in Tables S6–S9. Higher interaction energies for π(N)···π interactions are always observed for those with stronger M···π(N), such as those in MnPc, in which the π(N)···π interaction energies can reach as high as more than 7 kJ mol^{-1}. Such value is almost doubled if compared with the case of NiPc or H_2Pc. Additional insights have been shed to the nature of the interactions between intermolecular M–N pairs by looking into the electron density related properties,[23] including the Laplacian of electron density $\nabla^2\rho$, electron localization function (ELF), electrostatic potential (ESP), ellipticity ε, local energy density $H(r)$, eta index η and Mayer bond order (Figures S17–S20, Tables S6–S9). In the respective discussions, we focus on the planes formed by the intermolecular M–N pairs as well as BCPs and CPs between them. Detail discussions are performed in Section 12.2 of the Supporting Information. It is found that M–N interactions are of a closed-shell type, in which the Mn–N interaction has slightly shared interaction features. In addition, the interaction between M–N pairs in all MPc is mainly governed by electrostatic interactions. The trend of ESP charge on different M nucleus agrees with the trend for intermolecular distances and $E^{Dimer}_{int(BCP)}$, except for MnPc and FePc. For MnPc the slightly shared interaction features of Mn–N pairs play a role on top of the electrostatic interactions. As for FePc, the presence of CCPs between Fe–N pairs suggests repulsive interaction that partially counterpart the attractive interactions arising from the more positively charged Fe atoms. Besides ESP, the trend of Mayer bond order for intermolecular M–N pairs also agrees well with the trend for intermolecular distances and $E^{Dimer}_{int(BCP)}$ except for the Fe–N pairs, which may be explained by the same reasoning for the ESP owing to the presence of CCPs.

Besides the hole transfer integral, another critical factor that controls the charge transport properties is the coupling between charge carriers and vibrational modes in organic semiconductors. The calculated Huang–Rhys factors S listed in Table S5 suggest central metal atoms have a notable yet not significant impact towards the coupling strength between holes and specific vibrational modes in MPcs. However, in general, S values of H_2Pc and MPcs fall within the weak coupling regime. With further analysis into strongly coupled normal modes to holes as shown in Figure S21, it is interesting to notice that all MPcs with central metal atoms exhibit symmetric in-plane stretching modes while such vibrational symmetry is broken in H_2Pc, this can be related to similar HOMO distribution in these molecules as suggested in Figure S11. MnPc is slightly different from other MPcs as shown in Figure S21, in which the central pyrrole rings around Mn ion are likely to exhibit higher distortions in its positively charged state. This could be linked to a more unpaired singly occupied d orbital with their energy levels close to a_{1u} ligand HOMO in MnPc. In comparison, such distortion is most substantial in the outer phenyl rings in other MPcs as well as H_2Pc. In brief, the role of the central metal atoms may be twofold. In one way, they have a stronger impact towards hole transfer integrals through modulation of the intermolecular distances through the introduction of M···π(N) interactions depending on the occupation of d-states of the central metal atoms. Such effect becomes most notable when more singly occupied dz^2 orbital are available to participate in the interactions with π(N) orbital in neighboring MPcs molecules. On the other hand, they can also affect the hole-vibrational coupling of macrocycles due to different ligand bonds formed with the MPc rings. However, metal atoms exhibit less impact towards hole-vibrational coupling that is sensitive to molecular geometry and symmetry for the cases studied in this work, since no apparent geometry change occurs in these molecules except for H_2Pc.

In conclusion, single crystals of H_2Pc and MPcs are used to investigate the structure–property relationship. The single crystalline micro-ribbons of H_2Pc and MPcs are shown by TEM and SAED to grow along the shortest axis, the *b* axis. Single-crystal field-effect transistors show that the charge transport properties of MPcs mainly arise from the large π-plane of metal-free H_2Pc. Furthermore, on decreasing the intermolecular distances in H_2Pc and MPcs along their shortest packing axis, the hole mobilities gradually increase. The DFT based calculations in conjunction with the 1D polaron transport model give a good agreement with the experimentally measured trend. This trend of increasing hole mobility with decreasing intermolecular distance can be explained by increasing the hole transfer integral that is further related to stronger intermolecular interactions. Additional insights have been gained from the detail QTAIM, and NCI analysis, showing the coordination of different metal atoms into the H_2Pc planes can change the hole mobility via adjusting the intermolecular distances along the shortest axis through different M···π(N) interactions originating from metal d-orbital electronic configurations. The intermolecular π(N)···π interactions for the nearest neighbor atoms around M atoms also exhibit a strong dependence on the type of M atoms, thus eventually lead to the variation of overall interaction strength in MPcs. Detail analysis of the electron density properties reveals that the intermolecular M···N interactions are mainly closed-shell interactions in all MPcs, and are dominated by electrostatic interactions. However, weakly shared interaction features lead to significant increases in the Mn···N interactions, thus leading to much smaller intermolecular distances in MnPc ribbons. Other than the OFET applications that we demonstrate in this work, our results inspire us to think that single crystals of metal phthalocyanines may have potential applications in organic spintronics[24] and photocatalysis.[25]

Acknowledgements

H.J., D.F., and C.K. gratefully acknowledge the Singapore Ministry of Education for support via an AcRF Tier 1 grant (RG125/4) and an AcRF Tier 2 grant (MOE2014-T2-1-132). W.H. appreciates the financial support by the Ministry of Science and Technology of China (Grant Nos. 2017YFA0204503, 2016YFB0401100, 2013CB933403 and 2013CB933504), the National Natural Science Foundation of China (Grant Nos. 51633006, 91222203, 91233205 and 91433115), and the Chinese Academy of Sciences (Grant No. XDB12030300). P.H. and Long.Y. are partially supported by grants from the National Research Foundation, Prime Minister's Office, Singapore, under its Campus of Research Excellence and Technological Enterprise (CREATE) programme.

Conflict of interest

The authors declare no conflict of interest.

Keywords: charge transport · intermolecular interactions · organic field-effect transistors · organic single crystals · π stacking

How to cite: *Angew. Chem. Int. Ed.* **2018**, *57*, 10112–10117
Angew. Chem. **2018**, *130*, 10269–10274

[1] a) C. Wang, H. Dong, W. Hu, Y. Liu, D. Zhu, *Chem. Rev.* **2012**, *112*, 2208–2267; b) J.-L. Brédas, D. Beljonne, V. Coropceanu, J. Cornil, *Chem. Rev.* **2004**, *104*, 4971–5004; c) M. D. Curtis, J. Cao, J. W. Kampf, *J. Am. Chem. Soc.* **2004**, *126*, 4318–4328; d) H. Jiang, X. Yang, Z. Cui, Y. Liu, H. Li, W. Hu, C. Kloc, *CrystEngComm* **2014**, *16*, 5968–5983; e) H. Jiang, P. Hu, J. Ye, K. K. Zhang, Y. Long, W. Hu, C. Kloc, *J. Mater. Chem. C* **2018**, *6*, 1884–1902.

[2] R. Kubiak, J. Janczak, *J. Alloys Compd.* **1992**, *190*, 117–120.

[3] a) C. J. Brown, *J. Chem. Soc. A* **1968**, 2488–2493; b) A. Hoshino, Y. Takenaka, H. Miyaji, *Acta Crystallogr. Sect. B* **2003**, *59*, 393–403; c) P. Erk, H. Hengelsberg, M. F. Haddow, R. van Gelder, *CrystEngComm* **2004**, *6*, 474–483; d) R. Mason, G. A. Williams, P. E. Fielding, *J. Chem. Soc. Dalton Trans.* **1979**, 676–683; e) G. A. Williams, B. N. Figgis, R. Mason, S. A. Mason, P. E. Fielding, *J. Chem. Soc. Dalton Trans.* **1980**, 1688–1692; f) B. N. Figgis, E. S. Kucharski, P. A. Reynolds, *J. Am. Chem. Soc.* **1989**, *111*, 1683–1692; g) P. A. Reynolds, B. N. Figgis, E. S. Kucharski, S. A. Mason, *Acta Crystallogr. Sect. B* **1991**, *47*, 899–904; h) P. Ballirano, R. Caminiti, C. Ercolani, A. Maras, M. A. Orru, *J. Am. Chem. Soc.* **1998**, *120*, 12798–12807; i) W. R. Scheidt, W. Dow, *J. Am. Chem. Soc.* **1977**, *99*, 1101–1104; j) J. F. Kirner, W. Dow, W. R. Scheidt, *Inorg. Chem.* **1976**, *15*, 1685–1690; k) D. V. Konarev, M. Ishikawa, S. S. Khasanov, A. Otsuka, H. Yamochi, G. Saito, R. N. Lyubovskaya, *Inorg. Chem.* **2013**, *52*, 3851–3859; l) L. A. Rochford, D. S. Keeble, O. J. Holmes, G. J. Clarkson, T. S. Jones, *J. Mater. Chem. C* **2014**, *2*, 6056–6060; m) J. M. Robertson, I. Woodward, *J. Chem. Soc.* **1937**, 219–230; n) Y. Takahashi, K. Hayakawa, K. Takayama, S. Yokokura, J. Harada, H. Hasegawa, T. Inabe, *Chem. Mater.* **2014**, *26*, 993–998; o) B. N. Figgis, R. Mason, G. A. Williams, *Acta Crystallogr. Sect. B* **1980**, *36*, 2963–2970; p) B. N. Figgis, E. S. Kucharski, G. A. Williams, *J. Chem. Soc. Dalton Trans.* **1980**, 1515–1525.

[4] a) R. R. Sun, L. Wang, J. Tian, X. M. Zhang, J. Z. Jiang, *Nanoscale* **2012**, *4*, 6990–6996; b) I. Bruder, J. Schöneboom, R. Dinnebier, A. Ojala, S. Schäfer, R. Sens, P. Erk, J. Weis, *Org. Electron.* **2010**, *11*, 377–387; c) M. Grobosch, C. Schmidt, R. Kraus, M. Knupfer, *Org. Electron.* **2010**, *11*, 1483–1488; d) M. Gsänger, D. Bialas, L. Huang, M. Stolte, F. Würthner, *Adv. Mater.* **2016**, *28*, 3615–3645; e) O. A. Melville, B. H. Lessard, T. P. Bender, *ACS Appl. Mater. Interfaces* **2015**, *7*, 13105–13118; f) H. Lu, N. Kobayashi, *Chem. Rev.* **2016**, *116*, 6184–6261; g) G. de la Torre, C. G. Claessens, T. Torres, *Chem. Commun.* **2007**, 2000–2015.

[5] a) F. I. Bohrer, C. N. Colesniuc, J. Park, M. E. Ruidiaz, I. K. Schuller, A. C. Kummel, W. C. Trogler, *J. Am. Chem. Soc.* **2009**, *131*, 478–485; b) F. I. Bohrer, A. Sharoni, C. Colesniuc, J. Park, I. K. Schuller, A. C. Kummel, W. C. Trogler, *J. Am. Chem. Soc.* **2007**, *129*, 5640–5646; c) G. Guillaud, J. Simon, J. P. Germain, *Coord. Chem. Rev.* **1998**, *178*, 1433–1484; d) W. Huang, X. Zhuang, F. S. Melkonyan, B. Wang, L. Zeng, G. Wang, S. Han, M. J. Bedzyk, J. Yu, T. J. Marks, A. Facchetti, *Adv. Mater.* **2017**, *29*, 1701706.

[6] Y. Kitaoka, T. Sakai, K. Nakamura, T. Akiyama, T. Ito, *J. Appl. Phys.* **2013**, *113*, 17E130.

[7] a) M.-E. Ragoussi, J.-J. Cid, J.-H. Yum, G. de la Torre, D. Di Censo, M. Grätzel, M. K. Nazeeruddin, T. Torres, *Angew. Chem. Int. Ed.* **2012**, *51*, 4375–4378; *Angew. Chem.* **2012**, *124*, 4451–4454; b) V. P. Singh, R. S. Singh, B. Parthasarathy, A.

Aguilera, J. Anthony, M. Payne, *Appl. Phys. Lett.* **2005**, *86*, 082106.
[8] a) L. Li, Q. Tang, H. Li, X. Yang, W. Hu, Y. Song, Z. Shuai, W. Xu, Y. Liu, D. Zhu, *Adv. Mater.* **2007**, *19*, 2613 – 2617; b) A. Singh, A. Kumar, A. Kumar, S. Samanta, A. K. Debnath, P. Jha, R. Prasad, Z. Salmi, S. Nowak, M. M. Chehimi, D. K. Aswal, S. K. Gupta, *Appl. Phys. Lett.* **2012**, *101*, 222102 – 222105; c) S. Dong, C. Bao, H. Tian, D. Yan, Y. Geng, F. Wang, *Adv. Mater.* **2013**, *25*, 1165 – 1169; d) S. Samanta, D. K. Aswal, A. Singh, A. K. Debnath, M. S. Kumar, Y. Hayakawa, S. K. Gupta, J. V. Yakhmi, *Appl. Phys. Lett.* **2010**, *96*, 013305 – 013303; e) R. Zeis, T. Siegrist, C. Kloc, *Appl. Phys. Lett.* **2005**, *86*, 022103; f) X. Kong, X. Zhang, D. Gao, D. Qi, Y. Chen, J. Jiang, *Chem. Sci.* **2015**, *6*, 1967 – 1972; g) L. Huang, C. Liu, X. Qiao, H. Tian, Y. Geng, D. Yan, *Adv. Mater.* **2011**, *23*, 3455 – 3459.
[9] C. Lee, K. Sohlberg, *Chem. Phys.* **2010**, *367*, 7 – 19.
[10] M. Martin, J. J. Andre, J. Simon, *J. Appl. Phys.* **1983**, *54*, 2792 – 2794.
[11] K. Tabata, T. Sasaki, Y. Yamamoto, *Appl. Phys. Lett.* **2013**, *103*, 043301.
[12] M.-S. Liao, S. Scheiner, *J. Chem. Phys.* **2001**, *114*, 9780 – 9791.
[13] a) Z. Bao, A. J. Lovinger, A. Dodabalapur, *Appl. Phys. Lett.* **1996**, *69*, 3066 – 3068; b) R. D. Yang, T. Gredig, C. N. Colesniuc, J. Park, I. K. Schuller, W. C. Trogler, A. C. Kummel, *Appl. Phys. Lett.* **2007**, *90*, 263506; c) H. Gou, G. Wang, Y. Tong, Q. Tang, Y. Liu, *Org. Electron.* **2016**, *30*, 158 – 164; d) R. W. I. de Boer, A. F. Stassen, M. F. Craciun, C. L. Mulder, A. Molinari, S. Rogge, A. F. Morpurgo, *Appl. Phys. Lett.* **2005**, *86*, 262109; e) H. Jiang, P. Hu, J. Ye, Y. Li, H. Li, X. Zhang, R. Li, H. Dong, W. Hu, C. Kloc, *Adv. Mater.* **2017**, *29*, 1605053.
[14] a) I. G. Lezama, M. Nakano, N. A. Minder, Z. Chen, F. V. Di Girolamo, A. Facchetti, A. F. Morpurgo, *Nat. Mater.* **2012**, *11*, 788 – 794; b) M. Uno, T. Uemura, Y. Kanaoka, Z. Chen, A. Facchetti, J. Takeya, *Org. Electron.* **2013**, *14*, 1656 – 1662; c) K. Willa, R. Hausermann, T. Mathis, A. Facchetti, Z. Chen, B. Batlogg, *J. Appl. Phys.* **2013**, *113*, 133707; d) H. T. Yi, Z. Chen, A. Facchetti, V. Podzorov, *Adv. Funct. Mater.* **2016**, *26*, 2365 – 2370; e) H. Jiang, J. Ye, P. Hu, F. Wei, K. Du, N. Wang, T. Ba, S. Feng, C. Kloc, *Sci. Rep.* **2014**, *4*, 7573.
[15] a) Q. X. Tang, H. X. Li, M. He, W. P. Hu, C. M. Liu, K. Q. Chen, C. Wang, Y. Q. Liu, D. B. Zhu, *Adv. Mater.* **2006**, *18*, 65 – 68; b) Q. Tang, L. Jiang, Y. Tong, H. Li, Y. Liu, Z. Wang, W. Hu, Y. Liu, D. Zhu, *Adv. Mater.* **2008**, *20*, 2947 – 2951.
[16] J. Silver, C. S. Frampton, G. R. Fern, D. A. Davies, J. R. Miller, J. L. Sosa-Sanchez, *Inorg. Chem.* **2001**, *40*, 5434 – 5439.
[17] a) J. E. Norton, J. L. Bredas, *J. Chem. Phys.* **2008**, *128*, 034701; b) Z. Zhang, L. Jiang, C. Cheng, Y. Zhen, G. Zhao, H. Geng, Y. Yi, L. Li, H. Dong, Z. Shuai, W. Hu, *Angew. Chem. Int. Ed.* **2016**, *55*, 5206 – 5209; *Angew. Chem.* **2016**, *128*, 5292 – 5295; c) L. Q. Li, Q. X. Tang, H. X. Li, W. P. Hu, *J. Phys. Chem. B* **2008**, *112*, 10405 – 10410; d) S. Dong, H. Tian, L. Huang, J. Zhang, D. Yan, Y. Geng, F. Wang, *Adv. Mater.* **2011**, *23*, 2850 – 2854.
[18] H. Jiang, C. Kloc, *MRS Bull.* **2013**, *38*, 28 – 33.
[19] a) H. Jiang, K. J. Tan, K. K. Zhang, X. Chen, C. Kloc, *J. Mater. Chem.* **2011**, *21*, 4771 – 4773; b) Z. Bao, J. Locklin, *Organic Field-Effect Transistors*, Taylor & Francis, New York, **2007**; c) L. Bürgi, T. J. Richards, R. H. Friend, H. Sirringhaus, *J. Appl. Phys.* **2003**, *94*, 6129 – 6137; d) S. D. Wang, T. Minari, T. Miyadera, K. Tsukagoshi, Y. Aoyagi, *Appl. Phys. Lett.* **2007**, *91*, 203508.
[20] a) D. Chen, J. Ye, H. Zhang, Y. Zhao, *J. Phys. Chem. B* **2011**, *115*, 5312 – 5321; b) J. Ye, D. Chen, Y. Zhao, *J. Phys. Conf. Ser.* **2012**, *338*, 012018; c) D. A. da Silva Filho, V. Coropceanu, D. Fichou, N. E. Gruhn, T. G. Bill, J. Gierschner, J. Cornil, J. L. Bredas, *Philos. Trans. R. Soc. A* **2007**, *365*, 1435 – 1452.
[21] a) H. Jiang, P. Hu, J. Ye, A. Chaturvedi, K. K. Zhang, Y. Li, Y. Long, D. Fichou, C. Kloc, W. Hu, *Angew. Chem. Int. Ed.* **2018**, https://doi.org/10.1002/anie.201713288; *Angew. Chem.* **2018**, https://doi.org/10.1002/ange.201713288; b) T. Lu, F. W. Chen, *J. Comput. Chem.* **2012**, *33*, 580 – 592.
[22] a) A. Mugarza, R. Robles, C. Krull, R. Korytár, N. Lorente, P. Gambardella, *Phys. Rev. B* **2012**, *85*, 155437; b) A. J. Wallace, B. E. Williamson, D. L. Crittenden, *Can. J. Chem.* **2016**, *94*, 1163 – 1168.
[23] a) D. Cremer, E. Kraka, *Angew. Chem. Int. Ed. Engl.* **1984**, *23*, 627 – 628; *Angew. Chem.* **1984**, *96*, 612 – 614; b) B. Niepötter, R. Herbst-Irmer, D. Kratzert, P. P. Samuel, K. C. Mondal, H. W. Roesky, P. Jerabek, G. Frenking, D. Stalke, *Angew. Chem. Int. Ed.* **2014**, *53*, 2766 – 2770; *Angew. Chem.* **2014**, *126*, 2806 – 2811; c) N. J. M. Amezaga, S. C. Pamies, N. M. Peruchena, G. L. Sosa, *J. Phys. Chem. A* **2010**, *114*, 552 – 562.
[24] A. Atxabal, M. Ribeiro, S. Parui, L. Urreta, E. Sagasta, X. Sun, R. Llopis, F. Casanova, L. E. Hueso, *Nat. Commun.* **2016**, *7*, 13751.
[25] A. B. Sorokin, *Chem. Rev.* **2013**, *113*, 8152 – 8191.
[26] CCDC 1520127 (H_2Pc, 100 K), 1829924 (H_2Pc, 298 K), 1482761 (CuPc,100 K), 1830278 (CuPc,298 K), 1482845 (CoPc, 100 K), 1829930 (CoPc, 298 K), 1482758 (ZnPc, 100 K), 1829938 (ZnPc, 298 K), 1482844 (FePc, 100 K), 1829939 (FePc, 298 K), 1482846 (NiPc, 100 K), 1829940 (NiPc, 298 K), and 1520128 (MnPc, 100 K), 1829941 (MnPc, 298 K)contain the supplementary crystallographic data for this paper. These data can be obtained free of charge from The Cambridge Crystallographic Data Centre.

Manuscript received: March 20, 2018
Accepted manuscript online: May 14, 2018
Version of record online: June 21, 2018

